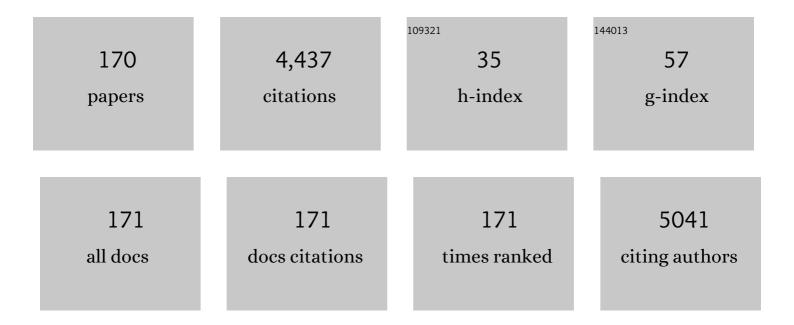
List of Publications by Year in descending order

Source: https://exaly.com/author-pdf/2585431/publications.pdf Version: 2024-02-01



#	Article	IF	CITATIONS
1	Co-Support Compound Formation in Alumina-Supported Cobalt Catalysts. Journal of Catalysis, 2001, 204, 98-109.	6.2	330
2	Synthesis of Au–ZnO and Pt–ZnO nanocomposites by one-step flame spray pyrolysis and its application for photocatalytic degradation of dyes. Catalysis Communications, 2009, 10, 1380-1385.	3.3	179
3	Effect of zirconia-modified alumina on the properties of Co/γ-Al2O3 catalysts. Journal of Catalysis, 2003, 215, 66-77.	6.2	132
4	Effects of synthesis conditions and annealing post-treatment on the photocatalytic activities of ZnO nanoparticles in the degradation of methylene blue dye. Chemical Engineering Journal, 2010, 164, 77-84.	12.7	131
5	Effect of strong metal–support interaction on the catalytic performance of Pd/TiO2 in the liquid-phase semihydrogenation of phenylacetylene. Journal of Catalysis, 2009, 262, 199-205.	6.2	118
6	CO Hydrogenation on Ru-Promoted Co/MCM-41 Catalysts. Journal of Catalysis, 2002, 211, 530-539.	6.2	104
7	Effect of TiO2 Crystalline Phase Composition on the Physicochemical and Catalytic Properties of Pd/TiO2 in Selective Acetylene Hydrogenation. Journal of Physical Chemistry B, 2006, 110, 8019-8024.	2.6	88
8	High-temperature flame spray pyrolysis induced stabilization of Pt single-atom catalysts. Applied Catalysis B: Environmental, 2021, 281, 119471.	20.2	85
9	Effect of Cobalt Precursors on the Dispersion of Cobalt on MCM-41. Catalysis Letters, 2003, 91, 95-102.	2.6	71
10	CO Hydrogenation on Ru-Promoted Co/MCM-41 Catalysts. Journal of Catalysis, 2002, 211, 530-539.	6.2	70
11	A comparative study of Pd/SiO2 and Pd/MCM-41 catalysts in liquid-phase hydrogenation. Catalysis Communications, 2004, 5, 583-590.	3.3	70
12	Effects of pH and pore characters of mesoporous silicas on horseradish peroxidase immobilization. Journal of Molecular Catalysis B: Enzymatic, 2009, 56, 246-252.	1.8	68
13	Dehydration of methanol to dimethyl ether over nanocrystalline Al2O3 with mixed Î <sup>3</sup> - and χ-crystalline phases. Catalysis Communications, 2008, 9, 1955-1958.	3.3	67
14	Selective hydrogenation of 1,3-butadiene over Pd and Pd–Sn catalysts supported on different phases of alumina. Catalysis Today, 2011, 164, 28-33.	4.4	67
15	Improvement of Pd/Al2O3 catalyst performance in selective acetylene hydrogenation using mixed phases Al2O3 support. Catalysis Communications, 2008, 10, 86-91.	3.3	66
16	Selective hydrogenation of acetylene in excess ethylene on micron-sized and nanocrystalline TiO2 supported Pd catalysts. Applied Catalysis A: General, 2006, 314, 128-133.	4.3	64
17	Effects of Pd precursors on the catalytic activity and deactivation of silica-supported Pd catalysts in liquid phase hydrogenation. Applied Catalysis A: General, 2005, 292, 322-327.	4.3	61
18	Impact of palladium silicide formation on the catalytic properties of Pd/SiO2 catalysts in liquid-phase semihydrogenation of phenylacetylene. Journal of Molecular Catalysis A, 2007, 261, 29-35.	4.8	61

#	Article	IF	CITATIONS
19	Transesterification of palm oil and esterification of palm fatty acid in near- and super-critical methanol with SO4–ZrO2 catalysts. Fuel, 2010, 89, 2387-2392.	6.4	60
20	Improvement of early cell adhesion on Thai silk fibroin surface by low energy plasma. Colloids and Surfaces B: Biointerfaces, 2013, 111, 579-586.	5.0	60
21	Modification of acid properties and catalytic properties of AlPO4 by hydrothermal pretreatment for methanol dehydration to dimethyl ether. Applied Catalysis A: General, 2010, 378, 119-123.	4.3	59
22	Characteristics and catalytic properties of Pt–Sn/Al2O3 nanoparticles synthesized by one-step flame spray pyrolysis in the dehydrogenation of propane. Applied Catalysis A: General, 2009, 370, 1-6.	4.3	58
23	Effect of crystallite size on the surface defect of nano-TiO2 prepared via solvothermal synthesis. Journal of Crystal Growth, 2006, 297, 234-238.	1.5	56
24	Selective hydrogenation of acetylene over Pd catalysts supported on nanocrystalline α-Al2O3 and Zn-modified α-Al2O3. Catalysis Communications, 2008, 9, 2297-2302.	3.3	52
25	A comparative study of strong metal–support interaction and catalytic behavior of Pd catalysts supported on micron- and nano-sized TiO2 in liquid-phase selective hydrogenation of phenylacetylene. Journal of Molecular Catalysis A, 2008, 279, 133-139.	4.8	51
26	Elucidation of the basicity dependence of 1-butene isomerization on MgO/Mg(OH)2 catalysts. Catalysis Communications, 2010, 12, 80-85.	3.3	50
27	Surface functionalized TiO2 supported Pd catalysts for solvent-free selective oxidation of benzyl alcohol. Catalysis Today, 2015, 250, 218-225.	4.4	45
28	Effect of nanoscale SiO2 and ZrO2 as the fillers on the microstructure of LLDPE nanocomposites synthesized via in situ polymerization with zirconocene. Materials Letters, 2007, 61, 1376-1379.	2.6	44
29	Effect of surface Ti3+ on the sol–gel derived TiO2 in the selective acetylene hydrogenation on Pd/TiO2 catalysts. Catalysis Today, 2015, 245, 134-138.	4.4	44
30	Characteristics and Catalytic Properties of Pd/SiO2 Synthesized by One-step Flame Spray Pyrolysis in Liquid-phase Hydrogenation of 1-Heptyne. Catalysis Letters, 2007, 119, 346-352.	2.6	43
31	Effect of quenching medium on photocatalytic activity of nano-TiO2 prepared by solvothermal method. Chemical Engineering Journal, 2008, 138, 622-627.	12.7	42
32	The liquid-phase hydrogenation of 1-heptyne over Pd–Au/TiO 2 catalysts prepared by the combination of incipient wetness impregnation and deposition–precipitation. Journal of Catalysis, 2013, 297, 155-164.	6.2	40
33	Effect of Ag addition on the properties of Pd–Ag/TiO2 catalysts containing different TiO2 crystalline phases. Catalysis Communications, 2007, 8, 2166-2170.	3.3	38
34	The low temperature selective oxidation of H2S to elemental sulfur on TiO2 supported V2O5 catalysts. Journal of Environmental Chemical Engineering, 2018, 6, 1414-1423.	6.7	38
35	Development of bimetallic Ni-Cu/SiO2 catalysts for liquid phase selective hydrogenation of furfural to furfuryl alcohol. Catalysis Communications, 2021, 149, 106221.	3.3	38
36	Preparation of Nano-Pd/SiO <sub>2</sub> by One-Step Flame Spray Pyrolysis and Its Hydrogenation Activities: Comparison to the Conventional Impregnation Method. Industrial & Engineering Chemistry Research, 2009, 48, 2819-2825.	3.7	37

#	Article	IF	CITATIONS
37	Performance of Pd catalysts supported on nanocrystalline α-Al2O3 and Ni-modified α-Al2O3 in selective hydrogenation of acetylene. Catalysis Today, 2008, 131, 553-558.	4.4	35
38	CO2 hydrogenation over Co/Al2O3 catalysts prepared via a solid-state reaction of fine gibbsite and cobalt precursors. Reaction Kinetics, Mechanisms and Catalysis, 2012, 107, 179-188.	1.7	35
39	Copper-modified alumina as a support for iron Fischer–Tropsch synthesis catalysts. Applied Catalysis A: General, 2007, 332, 130-137.	4.3	32
40	Preparation of improved Ag–Pd/TiO <sub>2</sub> catalysts using the combined strong electrostatic adsorption and electroless deposition methods for the selective hydrogenation of acetylene. Catalysis Science and Technology, 2016, 6, 5608-5617.	4.1	32
41	Formation of CoAl <sub><b>2</b></sub> O <sub><b>4</b></sub> Nanoparticles via Low-Temperature Solid-State Reaction of Fine Gibbsite and Cobalt Precursor. Journal of Nanomaterials, 2012, 2012, 1-8.	2.7	31
42	Variability of particle configurations achievable by 2-nozzle flame syntheses of the Au-Pd-TiO2 system and their catalytic behaviors in the selective hydrogenation of acetylene. Applied Catalysis A: General, 2018, 549, 1-7.	4.3	31
43	Synthesis of Cu/TiO2 catalysts by reactive magnetron sputtering deposition and its application for photocatalytic reduction of CO2 and H2O to CH4. Ceramics International, 2019, 45, 22961-22971.	4.8	31
44	NaOH modified WO3/SiO2 catalysts for propylene production from 2-butene and ethylene metathesis. Chinese Journal of Catalysis, 2014, 35, 232-241.	14.0	30
45	Effect of mixed Al2O3 structure between Î,- and α-Al2O3 on the properties of Pd/Al2O3 in the selective hydrogenation of 1,3-butadiene. Catalysis Communications, 2010, 11, 311-316.	3.3	29
46	Geometrical confinement effect in the liquid-phase semihydrogenation of phenylacetylene over mesostructured silica supported Pd catalysts. Catalysis Communications, 2011, 12, 910-916.	3.3	28
47	Effect of H2 partial pressure on surface reaction parameters during CO hydrogenation on Ru-promoted silica-supported Co catalysts. Journal of Catalysis, 2003, 213, 78-85.	6.2	27
48	The influence of Si-modified TiO2 on the activity of Ag/TiO2 in CO oxidation. Journal of Industrial and Engineering Chemistry, 2010, 16, 703-707.	5.8	27
49	Inhibition effect of Na+ form in ZSM-5 zeolite on hydrogen transfer reaction via 1-butene cracking. Catalysis Today, 2020, 358, 237-245.	4.4	27
50	Effect of transition metal dopants (M= Nb, La, Zr, and Y) on the M-TiO2 supported V2O5 catalysts in the selective oxidation of H2S to elemental sulfur. Journal of Environmental Chemical Engineering, 2018, 6, 5655-5661.	6.7	26
51	Impact of the Silica Support Structure on Liquid-Phase Hydrogenation on Pd Catalysts. Industrial & Engineering Chemistry Research, 2004, 43, 6014-6020.	3.7	25
52	Dependence of Quenching Process on the Photocatalytic Activity of Solvothermal-Derived TiO <sub>2</sub> with Various Crystallite Sizes. Industrial & Engineering Chemistry Research, 2008, 47, 693-697.	3.7	25
53	Characteristics and Catalytic Properties of Mesocellular Foam Silica Supported Pd Nanoparticles in the Liquid-Phase Selective Hydrogenation of Phenylacetylene. Catalysis Letters, 2011, 141, 1149-1155.	2.6	25
54	Liquid phase hydrogenation of phenylacetylene over Pd and PdZn catalysts in toluene: effects of alloying and CO2 pressurization. RSC Advances, 2014, 4, 24922.	3.6	25

#	Article	IF	CITATIONS
55	Effects of TiO2 structure and Co addition as a second metal on Ru-based catalysts supported on TiO2 for selective hydrogenation of furfural to FA. Scientific Reports, 2021, 11, 9786.	3.3	25
56	Improved catalytic performance of Pd/TiO2 in the selective hydrogenation of acetylene by using H2-treated sol–gel TiO2. Journal of Molecular Catalysis A, 2014, 383-384, 182-187.	4.8	24
57	One step synthesis of Pt–Co/TiO2 catalysts by flame spray pyrolysis for the hydrogenation of 3-nitrostyrene. Catalysis Communications, 2015, 61, 11-15.	3.3	24
58	Synthesis, Characterization, and Catalytic Properties of Pd and Pd–Ag Catalysts Supported on Nanocrystalline TiO2 Prepared by the Solvothermal Method. Catalysis Letters, 2005, 103, 53-58.	2.6	23
59	Application of Sulfonated Carbon-Based Catalyst for Reactive Extraction of 1,3-Propanediol from Model Fermentation Mixture. Industrial & Engineering Chemistry Research, 2010, 49, 12352-12357.	3.7	23
60	The effect of phosphorous precursor on the CO oxidation activity of P-modified TiO2 supported Ag catalysts. Catalysis Communications, 2010, 11, 1238-1243.	3.3	23
61	Effect of pretreatment atmosphere of WO <sub>x</sub> /SiO <sub>2</sub> catalysts on metathesis of ethylene and 2-butene to propylene. RSC Advances, 2018, 8, 11693-11704.	3.6	23
62	Mono- and bi-metallic Au–Pd/TiO2 catalysts synthesized by one-step flame spray pyrolysis for liquid-phase hydrogenation of 1-heptyne. Applied Catalysis A: General, 2013, 467, 132-141.	4.3	22
63	The effect of TiO2 particle size on the characteristics of Au–Pd/TiO2 catalysts. Catalysis Communications, 2015, 58, 70-75.	3.3	22
64	Microstructures and photocatalytic properties of ZnO films fabricated by Zn electrodeposition and heat treatment. Materials Science in Semiconductor Processing, 2018, 74, 232-237.	4.0	22
65	Effect of mixed γ- and χ-crystalline phases in nanocrystalline Al2O3 on the dispersion of cobalt on Al2O3. Catalysis Communications, 2008, 9, 207-212.	3.3	21
66	Glycothermal synthesis of nanocrystalline zirconia and their applications as cobalt catalyst supports. Materials Chemistry and Physics, 2005, 94, 207-212.	4.0	20
67	Effect of Ni-modified α-Al2O3 prepared by sol–gel and solvothermal methods on the characteristics and catalytic properties of Pd/α-Al2O3 catalysts. Materials Chemistry and Physics, 2008, 111, 431-437.	4.0	20
68	Lewis acid transformation to Bronsted acid sites over supported tungsten oxide catalysts containing different surface WOx structures. Catalysis Today, 2020, 358, 354-369.	4.4	20
69	Role of Al in Na-ZSM-5 zeolite structure on catalyst stability in butene cracking reaction. Scientific Reports, 2020, 10, 13643.	3.3	20
70	Enhanced Stability and Propene Yield in Propane Dehydrogenation on PtIn/Mg(Al)O Catalysts with Various In Loadings. Topics in Catalysis, 2018, 61, 1624-1632.	2.8	19
71	Formation of isolated tungstate sites on hierarchical structured SiO2- and HY zeolite-supported WOx catalysts for propene metathesis. Journal of Catalysis, 2019, 376, 150-160.	6.2	19
72	Effect of Support Crystallite Size on Catalytic Activity and Deactivation of Nanocrystalline ZnAl2O4-Supported Pd Catalysts in Liquid-Phase Hydrogenation. Catalysis Letters, 2008, 126, 313.	2.6	18

#	Article	IF	CITATIONS
73	Color improvment of C <sub>9</sub> hydrocarbon resin by hydrogenation over 2% Pd/γâ€alumina catalyst: Effect of degree of aromatic rings hydrogenation. Journal of Applied Polymer Science, 2010, 117, 2862-2869.	2.6	18
74	Influence of Crystallite Size of TiO2 Supports on the Activity of Dispersed Pt Catalysts in Liquid-Phase Selective Hydrogenation of 3-Nitrostyrene, Nitrobenzene, and Styrene. Catalysis Letters, 2015, 145, 606-611.	2.6	18
75	The key to catalytic stability on sol–gel derived SnOx/SiO2 catalyst and the comparative study of side reaction with K-PtSn/Al2O3 toward propane dehydrogenation. Catalysis Today, 2021, 375, 343-351.	4.4	18
76	Effect of nanocrystalline χ-Al2O3 structure on the catalytic behavior of Co/Al2O3 in CO hydrogenation. Catalysis Today, 2011, 164, 302-307.	4.4	17
77	Role of support nature (γ-Al2O3 and SiO2-Al2O3) on the performances of rhenium oxide catalysts in the metathesis of ethylene and 2-pentene. Journal of Natural Gas Chemistry, 2012, 21, 158-164.	1.8	17
78	Flame-made Pt/TiO2 catalysts for the liquid-phase selective hydrogenation of 3-nitrostyrene. Applied Catalysis A: General, 2015, 490, 193-200.	4.3	17
79	Effect of preparation method on the Pt-In modified Mg(Al)O catalysts over dehydrogenation of propane. Catalysis Today, 2020, 358, 100-108.	4.4	17
80	Flame spray-synthesized Pt-Co/TiO2 catalysts for the selective hydrogenation of furfural to furfuryl alcohol. Catalysis Communications, 2021, 149, 106246.	3.3	17
81	Influence of Preparation Method on the Nanocrystalline Porosity of α-Al <sub>2</sub> O <sub>3</sub> and the Catalytic Properties of Pd/α-Al <sub>2</sub> O <sub>3</sub> in Selective Acetylene Hydrogenation. Industrial & Engineering Chemistry Research, 2009, 48, 6273-6279.	3.7	16
82	Liquid-Phase Selective Hydrogenation of 1-Heptyne over Pd/TiO2 Catalyst Synthesized by One-Step Flame Spray Pyrolysis. Catalysis Letters, 2010, 136, 164-170.	2.6	16
83	Influence of flame conditions on the dispersion of Pd on the flame spray-derived Pd/TiO2 nanoparticles. Powder Technology, 2011, 210, 328-331.	4.2	16
84	A comparative study of liquid-phase hydrogenation on Pd/SiO2 in organic solvents and under pressurized carbon dioxide: Activity change and metal leaching/sintering. Journal of Molecular Catalysis A, 2006, 253, 20-24.	4.8	15
85	Production of propylene from an unconventional metathesis of ethylene and 2-pentene over Re2O7/SiO2-Al2O3 catalysts. Journal of Natural Gas Chemistry, 2012, 21, 83-90.	1.8	15
86	Effect of reduction temperature on the characteristics and catalytic properties of TiO2 supported AuPd alloy particles prepared by one-step flame spray pyrolysis in the selective hydrogenation of 1-heptyne. Applied Catalysis A: General, 2015, 506, 278-287.	4.3	15
87	Enhanced metathesis activity of low loading Re2O7/Al2O3 catalysts for propylene production by using aluminum nitrate as Al2O3 precursor. Applied Catalysis A: General, 2016, 517, 39-46.	4.3	15
88	An Alternative Correlation Equation between Particle Size and Structure Stability of Hâ^'Y Zeolite under Hydrothermal Treatment Conditions. Industrial & Engineering Chemistry Research, 2004, 43, 4066-4072.	3.7	14
89	Differences in characteristics and catalytic properties of Co catalysts supported on micron- and nano-sized zirconia. Catalysis Communications, 2006, 7, 192-197.	3.3	14
90	Effects of Co dopants and flame conditions on the formation of Co/ZrO2 nanoparticles by flame spray pyrolysis and their catalytic properties in CO hydrogenation. Catalysis Communications, 2011, 12, 917-922.	3.3	14

#	Article	IF	CITATIONS
91	Influence of preparation method on the catalytic performances of Re2O7/SiO2-Al2O3 catalysts in the metathesis of ethylene and 2-pentene. Journal of Industrial and Engineering Chemistry, 2014, 20, 145-152.	5.8	14
92	Comparative incorporation of Sn and In in Mg(Al)O for the enhanced stability of Pt/MgAl(X)O catalysts in propane dehydrogenation. Applied Catalysis A: General, 2021, 615, 118053.	4.3	14
93	Effect of Particle Size on the Hydrothermal Stability and Catalytic Activity of Polycrystalline Beta Zeolite. Journal of Porous Materials, 2005, 12, 293-299.	2.6	13
94	Synthesis of LLDPE/TiO2 nanocomposites by in situ polymerization with zirconocene/dMMAO catalyst: effect of [Al]/[Zr] ratios and TiO2 phases. Polymer Bulletin, 2011, 66, 479-490.	3.3	13
95	In situ-DRIFTS study: influence of surface acidity of rhenium-based catalysts in the metathesis of various olefins for propylene production. RSC Advances, 2017, 7, 38659-38665.	3.6	13
96	Effects of calcination and pretreatment temperatures on the catalytic activity and stability of H <sub>2</sub> -treated WO <sub>3</sub> /SiO <sub>2</sub> catalysts in metathesis of ethylene and 2-butene. RSC Advances, 2018, 8, 28555-28568.	3.6	13
97	Acidic nanomaterials (TiO <sub>2</sub> , ZrO <sub>2</sub> , and Al <sub>2</sub> O <sub>3</sub> ) are coke storage components that reduce the deactivation of the Pt–Sn/γ-Al <sub>2</sub> O <sub>3</sub> catalyst in propane dehydrogenation. Catalysis Science and Technology, 2020, 10, 5100-5112.	4.1	13
98	Observation of reduction on alkane products in butene cracking over ZSM-5 modified with Fe, Cu, and Ni catalysts. Fuel, 2021, 291, 120265.	6.4	13
99	Characterization of cobalt dispersed on the mixed nanoscale alumina and zirconia supports. Journal of Materials Processing Technology, 2008, 206, 352-358.	6.3	12
100	Effect of TiO2 Crystallite Size on the Activity of CO Oxidation. Catalysis Letters, 2009, 133, 76-83.	2.6	12
101	Effect of Nano-sized TiO2 Additional Support in WO3/SiO2 Catalyst Systems on Metathesis of Ethylene and Trans-2-Butene to Propylene. Catalysis Letters, 2013, 143, 919-925.	2.6	12
102	Comparative Effect of Nano-Sized ZrO2 and TiO2 Additional Supports in Silica-Supported Tungsten Catalysts on Performance in Metathesis of Ethylene and 2-Butene to Propylene. Catalysis Letters, 2014, 144, 1524-1529.	2.6	12
103	Hydrogen activated WOx-supported catalysts for Lewis acid transformation to Bronsted acid observed by in situ DRIFTS of adsorbed ammonia: Effect of different supports on the Lewis acid transformation. Catalysis Today, 2020, 358, 370-386.	4.4	12
104	Hydrogen and power generation via integrated bio-oil sorption-enhanced steam reforming and solid oxide fuel cell systems: Economic feasibility analysis. International Journal of Hydrogen Energy, 2021, 46, 11482-11493.	7.1	12
105	A study of alumina–zirconia mixed oxides prepared by the modified Pechini method as Co catalyst supports in CO hydrogenation. Applied Catalysis A: General, 2006, 303, 268-272.	4.3	11
106	Effect of SiO2–Al2O3 Composition on the Catalytic Performance of the Re2O7/SiO2–Al2O3 Catalysts in the Metathesis of Ethylene and 2-Pentene for Propylene Production. Catalysis Letters, 2012, 142, 1141-1149.	2.6	11
107	Deposition of Pt nanoparticles on TiO2 by pulsed direct current magnetron sputtering for selective hydrogenation of vanillin to vanillyl alcohol. Catalysis Today, 2020, 358, 51-59.	4.4	11
108	Highly active and stable Ni-incorporated spherical silica catalysts for CO2methanation. Catalysis Today, 2020, 358, 30-36.	4.4	11

#	Article	lF	CITATIONS
109	Flame sprayed tri-metallic Pt–Sn–X/Al2O3 catalysts (X = Ce, Zn, and K) for propane dehydration. Catalysis Communications, 2011, 12, 1161-1165.	3.3	10
110	Comparative Study of Lewis Acid Transformation on Non-reducible and Reducible Oxides Under Hydrogen Atmosphere by In Situ DRIFTS of Adsorbed NH3. Topics in Catalysis, 2018, 61, 1641-1652.	2.8	10
111	Effect of Surface Tungstate W5+ Species on the Metathesis Activity of W-Doped Spherical Silica Catalysts. Topics in Catalysis, 2018, 61, 1615-1623.	2.8	10
112	Electrochemical Evaluation of Corrosion Resistance of Trivalent Chromate Conversion Coatings with Different Organic Additives. ISIJ International, 2018, 58, 1316-1323.	1.4	10
113	The H2-Treated TiO2 Supported Pt Catalysts Prepared by Strong Electrostatic Adsorption for Liquid-Phase Selective Hydrogenation. Catalysts, 2018, 8, 87.	3.5	10
114	Preparation of aluminum magnesium oxide by different methods for use as PtSn catalyst supports in propane dehydrogenation. Catalysis Today, 2020, 358, 90-99.	4.4	10
115	Active Site Formation in WO <sub><i>x</i></sub> Supported on Spherical Silica Catalysts for Lewis Acid Transformation to BrÃ,nsted Acid Activity. Journal of Physical Chemistry C, 2020, 124, 15935-15943.	3.1	10
116	Growing 3D-nanostructured carbon allotropes from CO2 at room temperature under the dynamic CO2 electrochemical reduction environment. Carbon, 2022, 187, 241-255.	10.3	10
117	Metal-support interaction in mesoporous silica supported cobalt Fischer-Tropsch catalysts. Reaction Kinetics and Catalysis Letters, 2005, 85, 299-304.	0.6	9
118	Impact of Si and Zr addition on the surface defect and photocatalytic activity of the nanocrystalline TiO2 synthesized by the solvothermal method. Ceramics International, 2010, 36, 1439-1446.	4.8	9
119	Influence of micro- and nano-sized SiO2 excess support on the metathesis of ethylene and trans-2-butene to propylene over silica-supported tungsten catalysts. Reaction Kinetics, Mechanisms and Catalysis, 2014, 113, 225-240.	1.7	9
120	Effect of Dispersion of the Active Phase on the Activity and Coke Formation over WO3/SiO2 Catalysts in the Metathesis of Ethylene and 2-Butene. Catalysis Letters, 2015, 145, 1868-1875.	2.6	9
121	Preparation of \$\$hbox {TiO}_{2}\$\$ TiO 2 supported Au–Pd and Cu–Pd by the combined strong electrostatic adsorption and electroless deposition for selective hydrogenation of acetylene. Journal of Chemical Sciences, 2017, 129, 1721-1734.	1.5	9
122	Photocatalytic Liquid-Phase Selective Hydrogenation of 3-Nitrostyrene to 3-vinylaniline of Various Treated-TiO2 Without Use of Reducing Gas. Catalysts, 2019, 9, 329.	3.5	9
123	Characteristics and Catalytic Properties of Alumina–Zirconia Mixed Oxides Prepared by a Modified Pechini Method. Catalysis Letters, 2005, 103, 63-68.	2.6	8
124	Effect of Milling on the Formation of Nanocrystalline χâ€Al <sub>2</sub> O <sub>3</sub> from Gibbsite. Journal of the American Ceramic Society, 2010, 93, 3377-3383.	3.8	8
125	TRANSESTERIFICATION OF PALM OIL AT NEAR-CRITICAL CONDITIONS USING SULFONATED CARBON-BASED ACID CATALYST. Chemical Engineering Communications, 2013, 200, 1542-1552.	2.6	8
126	Comparison of the effects of χ phase- and Si- modified γ-Al2O3 supported Pt catalysts in CO oxidation. Catalysis Communications, 2014, 56, 92-95.	3.3	8

#	Article	IF	CITATIONS
127	CuAl2O4–CuO–Al2O3 catalysts prepared by flame-spray pyrolysis for glycerol hydrogenolysis. Molecular Catalysis, 2022, 523, 111426.	2.0	8
128	Effects of Si- and Y-modified nanocrystalline zirconia on the properties of Co/ZrO2 catalysts. Catalysis Communications, 2006, 7, 761-767.	3.3	7
129	Effects of impregnation solvent and reduction temperature on the catalytic performance of Pd/Al2O3 in the selective hydrogenation of 1,3-butadiene. Reaction Kinetics, Mechanisms and Catalysis, 2011, 103, 405-417.	1.7	7
130	Pd/TiO2 catalysts prepared by electroless deposition with and without SnCl2 sensitization for the liquid-phase hydrogenation of 3-hexyn-1-ol. Reaction Kinetics, Mechanisms and Catalysis, 2014, 111, 123-135.	1.7	7
131	Effect of N2O pretreatment on fresh and regenerated Pd-Ag $\hat{h}$ ±-Al2O3 catalysts during selective hydrogenation of acetylene. Reaction Kinetics and Catalysis Letters, 2007, 91, 195-202.	0.6	6
132	Impact of quenching process on the surface defect of titanium dioxide for hydrogen production from photocatalytic decomposition of water. Journal of Industrial and Engineering Chemistry, 2009, 15, 77-81.	5.8	6
133	Effect of Fe-modified α-Al2O3 on the properties of Pd/α-Al2O3 catalysts in selective acetylene hydrogenation. Reaction Kinetics and Catalysis Letters, 2009, 97, 115-123.	0.6	6
134	Improvement of propane oxidation activity over Pt/Al2O3 by the use of MIXED γ- and χ-Al2O3 supports. Reaction Kinetics, Mechanisms and Catalysis, 2010, 100, 441.	1.7	6
135	CHARACTERISTICS OF ACTIVATED CARBONS DERIVED FROM DEOILED RICE BRAN RESIDUES. Chemical Engineering Communications, 2013, 200, 1309-1321.	2.6	6
136	Liquid-Phase Hydrogenation of Phenylacetylene Over the Nano-Sized Pd/TiO <sub>2</sub> Catalysts. Journal of Nanoscience and Nanotechnology, 2014, 14, 3170-3175.	0.9	6
137	CO2 hydrogenation over FSP-made iron supported on cerium modified alumina catalyst. Catalysis Today, 2021, 375, 307-313.	4.4	6
138	Effect of the Nanostructured Zn/Cu Electrocatalyst Morphology on the Electrochemical Reduction of CO2 to Value-Added Chemicals. Nanomaterials, 2021, 11, 1671.	4.1	6
139	Formation and growth characteristics of nanostructured carbon films on nascent Ag clusters during room-temperature electrochemical CO <sub>2</sub> reduction. Nanoscale Advances, 2022, 4, 2255-2267.	4.6	6
140	Sugarcane Bagasse Ash as a Catalyst Support for Facile and Highly Scalable Preparation of Magnetic Fenton Catalysts for Ultra-Highly Efficient Removal of Tetracycline. Catalysts, 2022, 12, 446.	3.5	6
141	Effects of the support crystallite size and the reduction temperature on the properties of Pd/α-Al2O3 catalysts in selective acetylene hydrogenation. Reaction Kinetics and Catalysis Letters, 2008, 94, 233-241.	0.6	5
142	Tuning Pt dispersion and oxygen mobility of Pt/γ-Al2O3 by Si addition for CO oxidation. Reaction Kinetics, Mechanisms and Catalysis, 2016, 117, 565-581.	1.7	5
143	Influence of acidity on the performance of silica supported tungsten oxide catalysts assessed by in situ and Operando DRIFTS. Catalysis Today, 2020, 358, 345-353.	4.4	5
144	Sequential electrodeposition of Cu–Pt bimetallic nanocatalysts on boron-doped diamond electrodes for the simple and rapid detection of methanol. Scientific Reports, 2021, 11, 14354.	3.3	5

#	Article	IF	CITATIONS
145	Porous Electrodeposited Cu as a Potential Electrode for Electrochemical Reduction Reactions of CO2. Applied Sciences (Switzerland), 2021, 11, 11104.	2.5	5
146	Effect of TiO2 crystallite size on the dispersion of Co on nanocrystalline TiO2. Reaction Kinetics and Catalysis Letters, 2007, 91, 119-126.	0.6	4
147	Effect of N <sub>2</sub> pretreatment on the basicity, structural change, and isomerization activity of MgO and MgO/Mg(OH) <sub>2</sub> catalysts. Asia-Pacific Journal of Chemical Engineering, 2015, 10, 248-258.	1.5	4
148	Catalytic Cracking of Biodiesel Waste Using Metal Supported SBA-15 Mesoporous Catalysts. Catalysts, 2019, 9, 291.	3.5	4
149	Influence of surface Sn species and hydrogen interactions on the OH group formation over spherical silica-supported tin oxide catalysts. Reaction Chemistry and Engineering, 2020, 5, 1814-1823.	3.7	4
150	Catalytic performance of ZnO nanoparticle in formation of LLDPE/ZnO nanocomposites. Iranian Polymer Journal (English Edition), 2012, 21, 51-63.	2.4	3
151	LLDPE/TiO2 nanocomposites produced from different crystallite sizes of TiO2 via in situ polymerization. Science Bulletin, 2012, 57, 2177-2184.	1.7	3
152	One-step preparation of Pt–Ce and Pt–Sn–Ce/Al2O3 catalysts by flame spray pyrolysis in propane dehydrogenation. Reaction Kinetics, Mechanisms and Catalysis, 2014, 113, 149-158.	1.7	3
153	Propylsulfonic acid functionalized MCA cubic mesoporous and ZSM-5-MCA composite catalysts for anisole alkylation. Microporous and Mesoporous Materials, 2017, 239, 253-262.	4.4	3
154	Identification of extremely hard coke generation by low-temperature reaction on tungsten catalysts via Operando and in situ techniques. Scientific Reports, 2021, 11, 8071.	3.3	3
155	Deactivation of silica supported Pd catalysts during liquid-phase hydrogenation. Reaction Kinetics and Catalysis Letters, 2005, 86, 141-147.	0.6	2
156	Role of ruthenium in the reduction behavior of ruthenium-promoted cobalt/titania Fischer-Tropsch catalystsÂ. Reaction Kinetics and Catalysis Letters, 2006, 88, 65-71.	0.6	2
157	Characteristics and Catalytic Behavior of Pd Catalysts Supported on Nanostructure Titanate in Liquid-Phase Hydrogenation. Journal of Nanoscience and Nanotechnology, 2013, 13, 3062-3067.	0.9	2
158	Influence of autogeneous pressure under hydrothermal reaction on the structural and thermal stability of nanostructured titanates. Ceramics International, 2014, 40, 2323-2329.	4.8	2
159	Synthesis and Characteristics of CaO/MgO Mixed Oxides for the Double Bond Isomerization of 1-Butene. Journal of Nanoscience and Nanotechnology, 2018, 18, 439-444.	0.9	2
160	Differences in acid and catalytic properties of W incorporated spherical SiO2 and 1%Al-doped SiO2 in propene metathesis. Catalysis Today, 2020, , .	4.4	2
161	Metathesis of Ethylene and Trans-2-Butene over MgO Admixed WO3/SiO2 Catalysts. Engineering Journal, 2017, 21, 1-16.	1.0	2
162	Characteristics and catalytic properties of La-modified ZrO2 supported cobalt catalysts in CO hydrogenation. Reaction Kinetics, Mechanisms and Catalysis, 2011, 103, 367-378.	1.7	1

#	Article	IF	CITATIONS
163	Ethylene and mixed 2-butene cis/trans isomers metathesis: Influence of lanthanum as a second metal on the WO3/SiO2 catalysts. Korean Journal of Chemical Engineering, 2016, 33, 140-146.	2.7	1
164	Second metals (Lanthanum, Cerium, and Yttrium) modified W/SiO 2 catalysts for metathesis of ethylene and 2-butene. Catalysis Today, 2018, 309, 43-50.	4.4	1
165	Zirconia Modification on Nanocrystalline Titania-Supported Cobalt Catalysts for Methanation. Engineering Journal, 2012, 16, 29-38.	1.0	1
166	Liquid-Phase Selective Hydrogenation of Furfural to Furfuryl Alcohol over Ferromagnetic Element (Fe, Co, Ni, Nd)-Promoted Pt Catalysts Supported on Activated Carbon. Catalysts, 2022, 12, 393.	3.5	1
167	Effect of Si addition on the properties of nanocrystalline ZrO2-supported cobalt catalysts. Reaction Kinetics and Catalysis Letters, 2005, 87, 185-190.	0.6	0
168	Solvothermal-Derived Nanocrystalline TiO <sub>2</sub> Supported Co Catalysts in the Hydrogenation of Carbonmonoxide. Advanced Materials Research, 2013, 634-638, 595-598.	0.3	0
169	Metal (Fe, Co, Ni) supported on different aluminas as Fischer-Tropsch catalyst. AIP Conference Proceedings, 2015, , .	0.4	Ο
170	Aqueous-phase Selective Hydrogenation of Furfural to Furfuryl Alcohol over Ordered-mesoporous Carbon Supported Pt Catalysts Prepared by One-step Modified Soft-template Self-assembly Method. Journal of Oleo Science, 2022, , .	1.4	0